

ORIGINAL ARTICLE

Ageing-associated increase in SGLT2 disrupts mitochondrial/sarcoplasmic reticulum Ca^{2+} homeostasis and promotes cardiac dysfunction

Yusuf Olgar¹ | Erkan Tuncay¹ | Sinan Degirmenci¹ | Deniz Billur² | Rimpdy Dhingra³ | Lorrie Kirshenbaum³ | Belma Turan¹ 

¹Departments of Biophysics, Ankara University Faculty of Medicine, Ankara, Turkey

²Departments of Histology-Embryology, Ankara University Faculty of Medicine, Ankara, Turkey

³St. Boniface Hospital Albrechtsen Research Centre, Institute of Cardiovascular Sciences, University of Manitoba, Winnipeg, MB, Canada

Correspondence

Belma Turan, Departments of Biophysics, Ankara University Faculty of Medicine, Ankara, Turkey.
Email: belma.turan@medicine.ankara.edu.tr

Lorrie Kirshenbaum, Institute of Cardiovascular Sciences, St. Boniface Hospital Albrechtsen Research Centre, University of Manitoba, Winnipeg, MB, Canada.
Email: LKirshenbaum@sbr.ca

Funding information

This work was supported by grants (No. SBAG-216S979) from TUBITAK and COST action CA16225, Foundation grant to LAK from the Canadian Institute for Health Research, LAK is Canada Research Chair in Molecular Cardiology.

Abstract

The prevalence of death from cardiovascular disease is significantly higher in elderly populations; the underlying factors that contribute to the age-associated decline in cardiac performance are poorly understood. Herein, we identify the involvement of sodium/glucose co-transporter gene (SGLT2) in disrupted cellular Ca^{2+} -homeostasis, and mitochondrial dysfunction in age-associated cardiac dysfunction. In contrast to younger rats (6-month of age), older rats (24-month of age) exhibited severe cardiac ultrastructural defects, including deformed, fragmented mitochondria with high electron densities. Cardiomyocytes isolated from aged rats demonstrated increased reactive oxygen species (ROS), loss of mitochondrial membrane potential and altered mitochondrial dynamics, compared with younger controls. Moreover, mitochondrial defects were accompanied by mitochondrial and cytosolic Ca^{2+} ($[\text{Ca}^{2+}]_i$) overload, indicative of disrupted cellular Ca^{2+} -homeostasis. Interestingly, increased $[\text{Ca}^{2+}]_i$ coincided with decreased phosphorylation of phospholamban (PLB) and contractility. Aged-cardiomyocytes also displayed high $\text{Na}^+/\text{Ca}^{2+}$ -exchanger (NCX) activity and blood glucose levels compared with young-controls. Interestingly, the protein level of SGLT2 was dramatically increased in the aged cardiomyocytes. Moreover, SGLT2 inhibition was sufficient to restore age-associated defects in $[\text{Ca}^{2+}]_i$ -homeostasis, PLB phosphorylation, NCX activity and mitochondrial Ca^{2+} -loading. Hence, the present data suggest that deregulated SGLT2 during ageing disrupts mitochondrial function and cardiac contractility through a mechanism that impinges upon $[\text{Ca}^{2+}]_i$ -homeostasis. Our studies support the notion that interventions that modulate SGLT2-activity can provide benefits in maintaining $[\text{Ca}^{2+}]_i$ and cardiac function with advanced age.

KEYWORDS

ageing-heart, Ca^{2+} homeostasis, cardiovascular function, mitochondria, reactive oxygen species, sarcoplasmic reticulum, sodium/glucose cotransporter 2

This is an open access article under the terms of the Creative Commons Attribution License, which permits use, distribution and reproduction in any medium, provided the original work is properly cited.

© 2020 The Authors. *Journal of Cellular and Molecular Medicine* published by Foundation for Cellular and Molecular Medicine and John Wiley & Sons Ltd.

1 | INTRODUCTION

Over the past several decades, the average lifespan of humans has increased worldwide. Notably, the prevalence of death from cardiovascular disease is significantly higher in elderly populations.¹ The epidemiological and demographic results show the development of new therapies and interventions to mitigate the ageing-related decline in cardiac performance. Growing evidence suggests that ageing triggers cellular defects at the molecular and genetic levels which can result in organ dysfunction.² In this regard, both sarcoplasmic reticulum (SR) and mitochondrial dysfunctions have been linked to ageing-associated disorders including cardiac dysfunction and contractile failure.³

Mitochondrial function is essential for oxidative metabolism and ATP synthesis for maintaining tissue homeostasis and cell survival. Also, the mitochondrion serves as a platform for calcium regulation and programmed cell death by apoptosis and necrosis.^{4,5} Hence, the loss of normal mitochondrial function commonly associated with advanced age has been linked to abnormalities in sarcolemmal Ca^{2+} transport and alteration in action potential duration.^{3,6,7} However, the relationship between mitochondrial calcium handling defects and contractile dysfunction associated with ageing remains poorly understood.

Notably, we recently demonstrated that sodium/glucose co-transporter 2 (SGLT2), which is a member of the solute carrier family (SLC5A2) and is important in facilitating sodium-dependent glucose-transport and in the regulation of blood glucose levels, was significantly activated in the hearts of insulin-resistant animals with metabolic syndrome (MetS). Furthermore, we demonstrated that pharmacological inhibition of SGLT2 improved glucose tolerance and cardiac function.⁸ SGLT2 inhibitors have also been shown to provide clinical benefits in normalizing glucose levels and cardiac function in diabetic and non-diabetics patients with insulin resistance.^{9,10} While the underlying mechanisms by which SGLT2 inhibition confers cardioprotection are not well understood, several theories have been proposed including improved haemodynamics, more efficient metabolic function and cardiac/renal effects among others. In particular, a recent study by Pasternak et al¹⁰ demonstrated in the Scandinavian Cohort study that SGLT2 inhibitors significantly reduced the risk of heart failure and all-cause mortality, particularly in elderly patients. This finding raised awareness that SGLT2 inhibitors may play an important role in improving cardiac performance in the aged population. This view was substantiated by another recent study by Cintra et al,¹¹ who also showed beneficial effects of SGLT2 inhibition in elderly patients with heart diseases. At present, there are several theories that the underlying cardioprotection conferred by SGLT2 inhibition may converge on common signalling pathways that influence cardio-metabolic and bioenergetics involving Na^+/H^+ exchange-1, (NHE-1).¹²⁻¹⁴ Indeed, deregulated Na^+ and Ca^{2+} levels are early drivers of mitochondrial dysfunction, ROS production and cardiovascular morbidity and mortality.¹⁵ It has been shown that the increased intracellular Na^+ is an underlying cause of cardiac injury and metabolic dysfunction in diabetic cardiomyopathy, presumably

from elevated SGLT2 activity.^{14,16} In this regard, the studies have demonstrated that SGLT2 inhibition suppressed elevated NHE-1 activity and intracellular Na^+ levels in cardiomyocytes of diabetic animals.^{16,17} Despite our previous published work and clinical studies linking SGLT2 in the pathogenesis of cardiac dysfunction and heart failure, the underlying mechanism by which SGLT2 inhibition improves cardiac function in the aged myocardium remains poorly understood. Therefore, in the present study, we explored the mechanism by which SGLT2 disrupts cardiac function associated with advanced age. Given that the mitochondria are a major nodal point in the regulation of cardiac metabolism and intracellular Ca^{2+} ($[\text{Ca}^{2+}]_i$), we explored the impact of SGLT2 on mitochondrial Ca^{2+} homeostasis in young and aged cardiac myocytes. Our data provide new important information that SGLT2 disrupts mitochondrial/SR Ca^{2+} -homeostasis and thereby promotes cardiac dysfunction by impairing mitochondrial energy metabolism.

2 | MATERIALS AND METHODS

2.1 | Experimental animals

Our experimental protocols and all animal procedures are in coincidence with the guidelines of the Directive 2010/63/EU of the European Parliament on the protection of animals used for scientific purposes and are approved by Ankara University (reference # 2016-18-165).

Wistar male rats were grouped as 24-month-old (Aged group) vs. 6-month-old (Young group) and parameters such as blood glucose levels were analysed as described previously.⁸ Hearts were rapidly excised following anaesthesia with sodium pentobarbital (30 mg/kg bodyweight).

2.2 | Cardiomyocytes isolation

Cardiomyocytes isolation was performed from the left ventricles of hearts, as described previously.⁸ Briefly, hearts were cannulated in a Langendorff-perfusion system, followed by digestion with 1-mg/mL collagenase (Type IV, Worthington, USA) for 30-35 minutes. Cardiomyocytes were treated with either 100 nmol/L SGLT2 inhibitor (SGLT2i, dapagliflozin, D185360; for 4-5 hours at 37°C) or 0.1 $\mu\text{mol/L}$ MitoTEMPO for further experiments.

2.3 | Measurement of mitochondrial superoxide production and Ca^{2+} level by flow cytometry

To determine the mitochondrial superoxide level ($[\text{SOX}]_{\text{Mit}}$), isolated cardiomyocytes were incubated with 2.5- $\mu\text{mol/L}$ MitoSOX Red for 30-minutes at room temperature and cells were washed twice in PBS. Fluorescent intensity was measured by flow cytometry, and data were plotted as dot plots.¹⁸

The mitochondrial Ca^{2+} level ($[\text{Ca}^{2+}]_{\text{Mit}}$) was measured by incubating cardiomyocytes with 4- $\mu\text{mol/L}$ Fluo4-AM Ca^{2+} dye for 45-minutes at room temperature in extracellular solution contains (in mmol/L) 156 NaCl, 3 KCl, 2 MgSO_4 , 1.25 KH_2PO_4 , 10 D-glucose, 2 CaCl_2 and 10 HEPES, at pH 7.35. Cardiomyocytes are washed with PBS twice and incubated with intracellular solution contains (in mmol/L); NaCl 6, KCl 130, MgCl_2 7.8, KH_2PO_4 1, CaCl_2 0.4, EGTA 2, EDTA 10, malate 2, glutamate 2, ADP 2 and HEPES 20, at pH 7.1 solution including digitonin (25 mg/mL) and thapsigargin (10- $\mu\text{mol/L}$) for 10-minutes at room temperature. Real-time measurement of the fluorescence emission from each sample is reported as dot plots measuring the percentage of stained cells with Fluo-4AM fluorescence.¹⁹

To validate the mitochondrial membrane integrity under control during measurements, we directly measured the mitochondria Ca^{2+} level but not in the mitochondrial intermembrane space, all experiments were performed in cells under same experimental conditions (using Fluo-4AM and TMRM loaded permeabilized cells, by flow cytometry) through the determination of mitochondrial Ca^{2+} level and mitochondrial membrane potential (MMP), simultaneously by using confocal microscopy (see Appendix S1 and Figure S1).

2.4 | Measurement of mitochondrial membrane potential

The mitochondrial membrane potential in cardiomyocytes was measured with a fluorescence-based assay as described previously.²⁰ Briefly, a membrane-permeant single wavelength fluorescence dye JC-1 (5- $\mu\text{mol/L}$, 30-minutes) loaded cells were imaged with a confocal fluorescence microscope (Leica TCS SP5). Carbonyl cyanide 4-(trifluoromethoxy) phenylhydrazone (FCCP; 5- $\mu\text{mol/L}$) was used as a positive control for mitochondrial depolarization (MMP).

2.5 | Measurements of the resting levels of intracellular ions and global transient intracellular Ca^{2+} -changes

The basal levels of intracellular free Ca^{2+} , Na^+ and H^+ (or intracellular pH) levels ($[\text{Ca}^{2+}]_i$, $[\text{Na}^+]_i$, $[\text{H}^+]_i$) were measured in resting cardiomyocytes loaded with ion-specific fluorescence dyes (4- $\mu\text{mol/L}$ Fura-2AM for Ca^{2+} , 10- $\mu\text{mol/L}$ SBFI for Na^+ and 5- $\mu\text{mol/L}$ SNARF-1 for H^+). Fluorescence values were recorded by the use of a ratio-metric micro-spectrofluorometer (PTI Ratio master and FELIX software; Photon Technology International, Inc, NJ USA) for Ca^{2+} or a laser scanning microscope (confocal microscopy, Leica TCS SP5, Germany) for Na^+ , as described previously.⁸

To determine the intracellular transient Ca^{2+} -changes (Ca^{2+} -transients) in cardiomyocytes (loaded with Fura-2AM, 4- $\mu\text{mol/L}$), an electric-field stimulation (with a 10-ms duration electrical pulses at a frequency of 0.2 Hz) was applied. We took into consideration the potential influences of a temperature-dependent effect on lowered amplitude of intracellular Ca^{2+} -changes without changes in the time course

of measurements,^{21,22} as well as the potential effects of temperature on Ca^{2+} -sensitive fluorescent probes,²³ we used room temperature for both cell-loading and recordings from loaded cells. Therefore, fluorescence intensity changes were measured at room temperature by using the micro-spectrofluorometer (PTI, Lawrenceville, NJ, USA) and FELIX software, as described, previously.⁸

2.6 | Patch-clamp experiments

Electrophysiological parameters of cardiomyocytes were recorded by using the Axoclamp patch-clamp amplifier (Axopatch 200B amplifier, Axon Instruments, USA) at room temperature ($23 \pm 2^\circ\text{C}$). Cardiomyocytes were sampled and digitized at 5 kHz using an analog-to-digital converter and a software (Digidata 1200A and pCLAMP 10.0; Axon Instruments, USA). The amplifier has been used for either voltage-clamp mode (voltage-dependent K^+ -channel currents, I_K) or current-clamp mode (action potentials) to measure either ionic fluxes or membrane voltage changes, respectively, as described previously.⁸

Action potential duration from the repolarization phase at 25, 50, 75, 90% (APD_{25} , APD_{50} , APD_{75} , APD_{90}), the resting membrane potential, and the maximum amplitude of action potentials were calculated from original records (at least 15-20 records/cell).

The Na^+/K^+ -pump (NaK) current (I_{NaK}) was measured in freshly isolated left ventricular cardiomyocytes, as described previously.²⁴ Briefly, NaK inhibition was achieved by 20-minutes perfusion with 0- K^+ solution: NaCl 136, BaCl_2 2, MgCl_2 1, glucose 10, HEPES 5, NiCl_2 5 ve TrisCl 4 (mmol/L) (at pH = 7.4). To activate NaK , cardiomyocytes were reperfused with normal 4 K^+ solution: (NaCl 140, KCl 4, CaCl_2 2, MgCl_2 1, glucose 10 and HEPES, at pH = 7.4). The holding potential was -30 mV during the experiment.

The $\text{Na}^+/\text{Ca}^{2+}$ -exchanger (NCX) current was measured as described elsewhere.²⁵ The total NCX current (both inward and outward), I_{NCX} , was obtained from protocol composed of descending ramp from +80 to -120 mV at 0.1 mV/ms while holding potential was -40 mV. The external solution consisted of NaCl 130, TEA-Cl 10, Na-Hepes 11.8, MgCl_2 0.5, CaCl_2 1.8, ryanodine 0.005, nifedipine 0.02, glucose 10; pH 7.4 and the pipette solution CsCl 65, CaCl_2 10.92, EGTA 20, HEPES 10, MgATP 5, MgCl_2 0.5, TEA-Cl 20 and at pH 7.2.

2.7 | Measurement of cellular ATP level

The cellular level of ATP in isolated left ventricular cardiomyocytes was measured using a colorimetric ATP assay kit (Abcam, ab83355) with some modification, as described previously.⁸

2.8 | Histological analysis of cardiomyocytes

Electron microscopy was performed in cardiomyocytes, as described previously.²⁰ Ultra-thin sections were stained with uranyl

acetate and lead citrate and cells were observed using an LEO 906 E TEM (80 kV, Oberkochen, Germany). A Sharpey CCD and Image SP (Germany) digital imaging system were used to photograph.

To quantify the results, the mitochondrial aspect ratio as the ratio of length to width was calculated by using Image SP, the randomly selected five longitudinally arranged micrographs, as described previously.²⁶ For each cell, the lengths of 500 to 600 interfibrillar mitochondria were assessed, as described previously.²⁷

2.9 | Western-blot analysis

The protein samples were prepared from the cells and tissues as previously described.²⁰ Equal amount of cardiac cell lysates were run on SDS-polyacrylamide gels and incubated with antibodies against proteins Mfn1 (sc-166644, 1:1000), Mfn2 (sc-100560, 1:1000), Drp1 (sc-271583, 1:500), SERCA2 (SC-376235, 1:500), NCX (Santa Cruz, sc-12972), phospho-phospholamban-Ser¹⁶ (pPLB; sc-17024, 1:10 000), phospholamban (PLB; sc30142, 1:1000), SGLT2 (ab37296,1:1000). β -actin (Santa Cruz, sc-47778, 1:5000) and GAPDH (Cell Signaling, D16H11, 1/5000) were used as housekeeping proteins to detect equal protein loading.

Immunoreactive bands were detected by a chemiluminescent reaction (ECL kit, Amersham Pharmacia, USA). The densities of the bands are analysed using ImageJ software, and the results were presented as fold changes.

2.10 | QRT-PCR analysis

The mRNA levels were measured as described previously¹. The fold changes in the genes were analysed based on the comparative ($2^{-\Delta\Delta Ct}$) method. Primer sequence for SGLT2 is TCATTGCCGCGTATTTCTG (forward) and AACACCACAAAGAGCGCATT (reverse).

2.11 | Reagents and statistical analysis

Chemicals were obtained from Sigma-Aldrich (St. Louis, MO) unless otherwise stated. Data were collected from different myocyte isolations. Data are presented as Mean \pm SEM of at least three independent observations for Western blotting with GraphPad Prism 6.0 (GraphPad software, Inc, La Jolla, CA). To provide better presentation and distribution of Western blot data in terms of median and

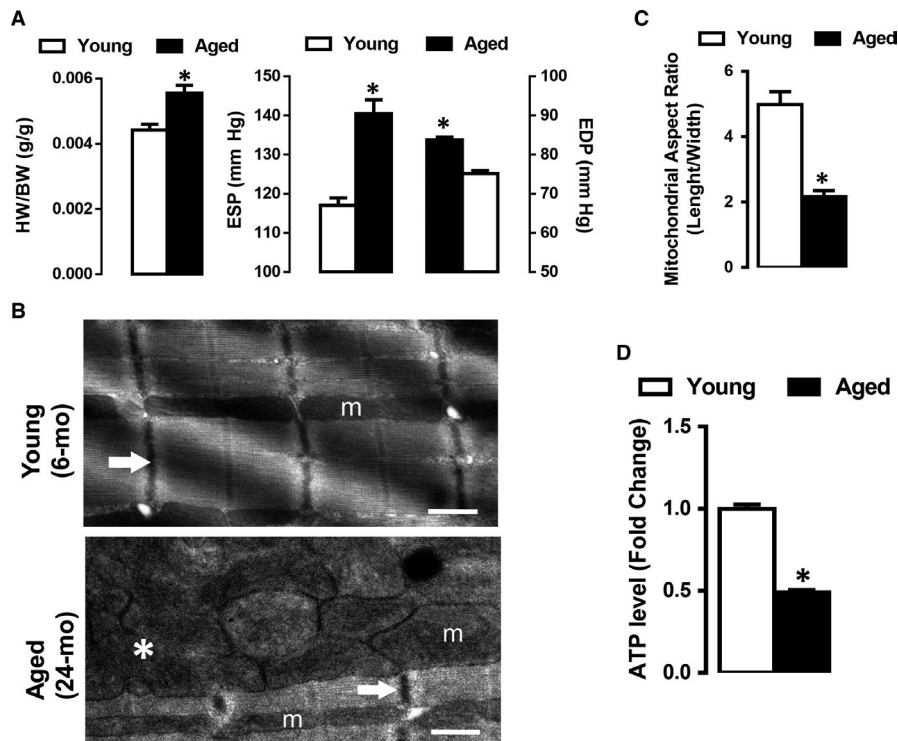


FIGURE 1 Altered myocardial ultrastructure and defective mitochondria in aged rats hearts. Panel A (Left): The ratio of heart weight to bodyweight in the young group (6 mo old, $n = 30$) and aged group (24 mo old, $n = 30$ rats). (Right): End-systolic (ESP) and end-diastolic blood pressure (EDP) in young and aged groups. Panel B: Representative transmission electron micrographs (EM) of ventricular cardiomyocytes from young (Top) and aged (Bottom) rat's heart. Normal myocardial ultrastructure with organized mitochondria in young group vs disrupted sarcomeres, unorganized and fragmented mitochondria in the aged group (magnification $\times 7750$). The symbols demonstrate; m for mitochondria, the arrow for Z-line, asterisk for fragmented mitochondrion. Panel C: Histogram depicts mitochondrial aspect ratio (length/width), from the data derived from EM shown in panel B. (Note: low mitochondrial aspect values are indicative of smaller and fragmented mitochondria). Panel D: Histogram presents fold change in ATP levels (young vs aged group), measured by colorimetric assay. Data are presented as Mean \pm SEM, statistical significance $^*P < 0.05$ vs. young group

interquartile range, we used a box and whisker graph. Comparisons between quantitative variables were assessed by the unpaired two-sided Student's *t* test at the $P < 0.05$ significance level.

3 | RESULTS

3.1 | Altered myocardial ultrastructure and cardiac function in aged hearts

To gain insight into the effects of ageing on cardiac dysfunction, we first determined whether the aged hearts (24 months) are hypertrophic and different from younger animals (6 months). As shown in Figure 1 panel A (Left panel), the heart weight to bodyweight ratio was significantly higher in the aged group compared with the corresponding young group. Further, end-systolic pressure (ESP) and end-diastolic blood pressure level (EDP) were higher in the aged group compared with the younger animal group, Figure 1 panel A (Right panel).

Also, we examined cardiac morphology by electron microscopy to examine ultrastructure and subcellular changes in the myocardium with ageing. Electron microscopy analysis revealed that in contrast to young animals, which displayed normal sarcomeric architecture and organized elongated mitochondria, severe ultrastructural defects characterized by damaged myofibrils, disorganized and fragmented mitochondria accompanied by a dilatation of SR T-tubules were observed in the aged hearts, Figure 1 panel B.

Further, a significant decrease in mitochondrial aspect ratio was observed in the aged hearts, indicative of increased mitochondrial fragmentation, Figure 1 panel C. Moreover, altered mitochondrial morphology coincides with a marked decline in ATP levels, Figure 1 panel D.

3.2 | Age-associated increase in reactive oxygen species (ROS) underlies mitochondrial defects

As we observed a decline in mitochondrial ATP in aged animals, suggesting that mitochondrial perturbations may be associated with contractile dysfunction. We used mitochondria targeting antioxidant (MitoTEMPO) that we have previously shown to reduce ROS level in the ventricular cardiomyocytes,²⁰ we assessed the effects of ageing on mitochondrial superoxide production in MitoSOX-loaded cardiomyocytes followed by flow cytometry analysis. As shown in Figure 2 panel A, the fluorescence intensity of MitoSOX was fourfold higher in the aged cardiomyocytes compared with cardiomyocytes from young hearts. Moreover, antioxidant MitoTEMPO exerted a protective effect against ageing-induced mitochondrial superoxide production, Figure 2 panel A.

As our previous studies demonstrated a role for mitochondrial redox signalling (via increases in ROS level) in the aetiology of ageing-associated organ dysfunction,²⁸ we determined the effect of MitoTEMPO treatment on mitochondrial membrane potential

(MMP) in isolated JC-1-loaded cardiomyocytes (Figure 2 panel B, original records in the left). The mitochondria were significantly depolarized in the aged cardiomyocytes, which was rescued by MitoTEMPO; FCCP was used as a positive control in the study, Figure 2 panel B.

Taking into consideration the essential processes of mitochondria fidelity such as mitochondrial dynamism (fusion and fission), we determined the expression levels of the mitochondrial fusion and fission proteins in the aged cardiomyocytes compared with young hearts in the absence and presence of MitoTEMPO. As shown by Western blot analysis in Figure 2 panel C, in contrast to Mitofusin 1 (Mfn1), Mitofusin 2 (Mfn2) expression was significantly decreased in cardiac myocytes of aged hearts. Furthermore, a marked increase in mitochondrial fission protein Drp1 was observed in aged cardiomyocytes, Figure 2 panel D. These data are consistent with increased mitochondrial fragmentation and reduced mitochondrial aspect ratio in the aged cardiomyocytes. Interestingly, MitoTEMPO treatment suppressed age-associated alterations in Mfn2 and Drp1 (Figure 2 panels C,D), suggesting that increased ROS production underlies mitochondrial perturbations and fragmentation associated with the aged hearts.

3.3 | Effects of ageing on intracellular Ca^{2+} signalling in ventricular cardiomyocytes

Elevated mitochondrial Ca^{2+} level ($[Ca^{2+}]_{Mit}$) has been identified as a major activator of mitochondrial permeability transition pore (mPTP) opening.²⁹ Among other potential influences of mPTP opening, cellular $[Ca^{2+}]_i$ is considered to be a major determinant of mPTP opening. As ageing alters $[Ca^{2+}]_i$ handling in cardiomyocytes,³⁰ we determined whether mitochondrial Ca^{2+} , $[Ca^{2+}]_{Mit}$ is elevated in the aged cardiomyocytes. As shown in Figure 3 panel A, (by flow cytometry), $[Ca^{2+}]_{Mit}$ was increased by 50% in aged cardiomyocytes compared with those of young cardiomyocytes. To verify the detrimental effect of ageing on depressed contractile activity, we mimicked the action potentials (APs) of age with electrical-field stimulation of cardiomyocytes and determined the transient changes of $[Ca^{2+}]_i$ (global $[Ca^{2+}]_i$ transients) in Fura-2AM loaded aged cardiomyocytes. As shown in Figure 3 panel B, the averaged peak amplitude (as $\Delta F_{340/380}$) of $[Ca^{2+}]_i$ transients were significantly smaller in the aged group compared with the younger group (Figure 3 panel B). Besides, the time to peak amplitude and the half time for recovery of Ca^{2+} transients in the aged group was significantly longer than those of the young group (Figure 3 panel C).

To test whether the $[Ca^{2+}]$ content of the sarcoplasmic reticulum (SR) could be altered with ageing, we performed further experiments using caffeine to assess SR Ca^{2+} extrusion. The responses to acute caffeine (10-mmol/L) were significantly lower in the aged group compared with the corresponding young group (Figure 3 panel D). To characterize the underlying mechanisms for altered Ca^{2+} transients, we monitored the protein expression of total and phosphorylated phospholamban

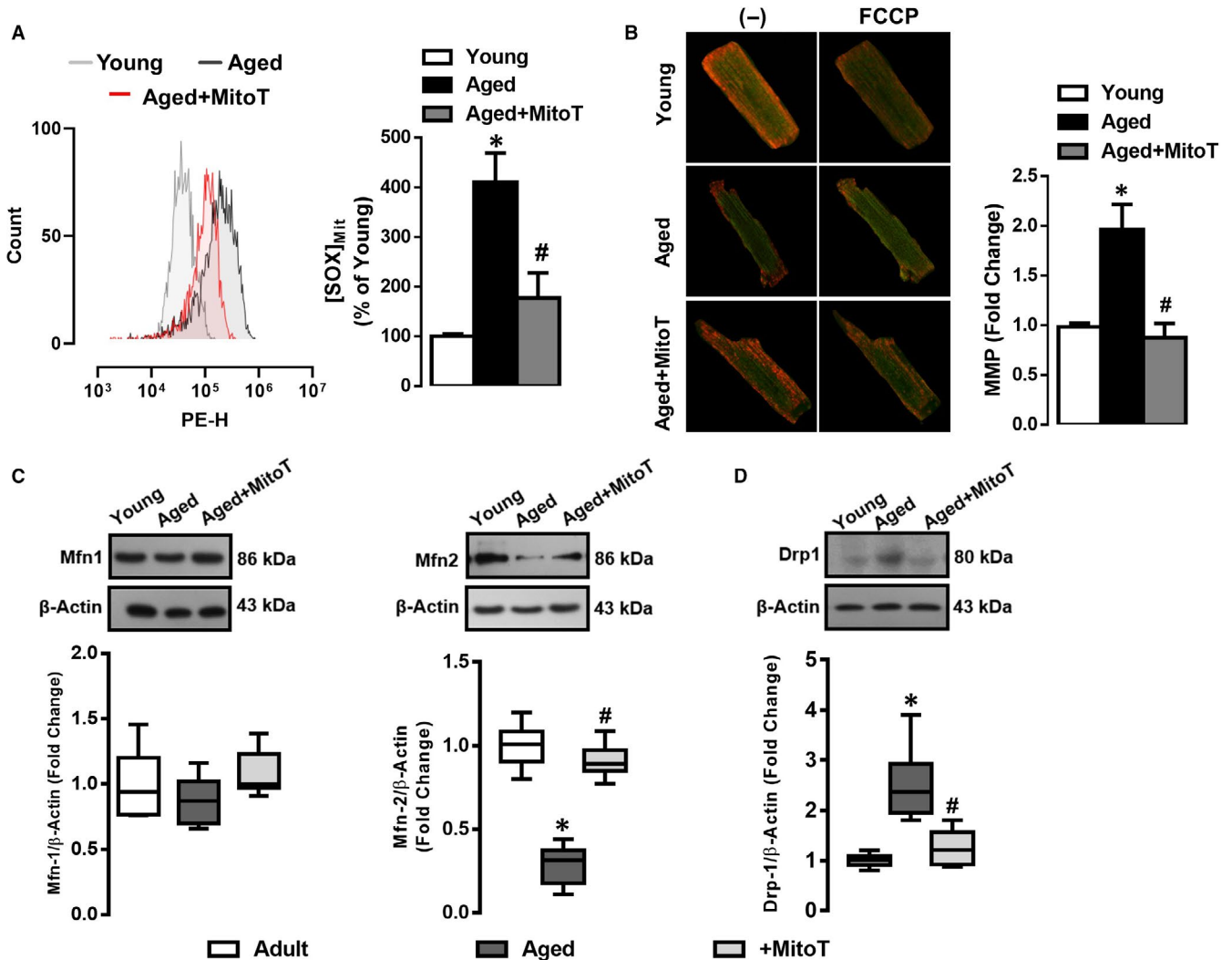


FIGURE 2 Increased mitochondrial reactive oxygen species (ROS) underlies the loss of mitochondrial membrane potential and altered dynamics in aged cardiomyocytes. Panel A (Left panel): Representative flow cytometric images (left) depicting mitochondrial superoxide $[SOX]_{Mit}$ production in cardiomyocytes loaded with MitoSOX (2.5- μ mol/L for 30-min at 37°C) for the groups (young, aged and aged + MitoTEMPO), as shown in the labels. Note: MitoTEMPO is a mitochondria-targeting antioxidant,²⁰ treated at 0.1- μ mol/L for 4-5 h at 37°C. Right panel: Histogram presenting per cent (%) change in values of $[SOX]_{Mit}$; Data are normalized to young controls. Panel B (Left panel): Representative fluorescent images for mitochondrial membrane potential (MMP) in JC-1 loaded cardiomyocytes, Right panel: Histogram presents fold change in MMP (young vs aged group). Note: Green colour marks loss of mitochondrial membrane potential. Data are presented as Mean \pm SEM, statistical significance * $P < 0.05$ vs. young group, # $P < 0.05$ vs. aged group. Panel C (Top panel): Western blot analysis of mitochondrial fusion proteins (Mfn1 and Mfn2); Bottom panel: Histogram presents fold change in Mfn1 and Mfn2 proteins. Panel D (Top panel): Western blot analysis for mitochondrial fission protein, Drp1 (D), Bottom: Histogram presents fold change in Drp1 protein. Actin serves as a housekeeping gene. All data are presented, as Mean \pm SEM. Cardiomyocytes were isolated from 5-6 rats/groups. Statistical significance $P < 0.05$ vs. young group, # $P < 0.05$ vs. aged group, statistical significance analysed by unpaired two-sided Student's t test

(pPLB), which modulates the SR Ca^{2+} -ATPase (SERCA) function. As shown in Figure 3 panels E,F, a marked decrease in phosphorylation of PLB (pPLB) was observed in aged cardiomyocytes.

3.4 | Ageing up-regulates SGLT2 and disrupts the intracellular ionic balance of cardiomyocytes

As action potential durations were prolonged in aged cardiomyocytes, we assessed whether intracellular ionic levels were altered

in aged cardiomyocytes. To test this possibility, we assessed changes in the Na^{+} -influx (via voltage-dependent Na^{+} channel current, I_{Na}) and Ca^{2+} -influx (via voltage-dependent L-type Ca^{2+} -channel currents, I_{CaL}) on the AP characteristics. However, there was no significant change in any parameter of the channel currents between young and aged groups (Figure S1 and Figure S2, panels A,B).

Next, we tested the resting levels of cytosolic Ca^{2+} ($[Ca^{2+}]_i$), measured by fluorescence microscopy by Fura-2 AM. As shown in Figure 4 panel A, cytosolic Ca^{2+} was found to be significantly

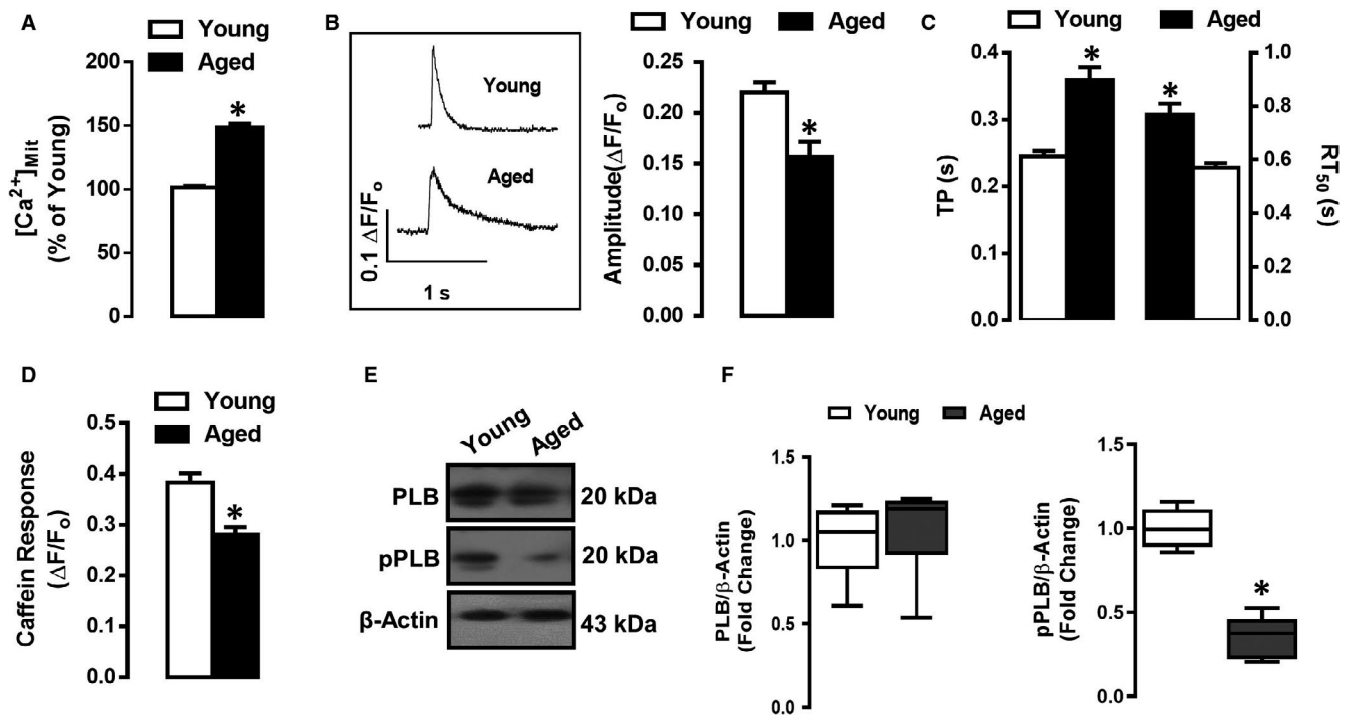


FIGURE 3 Ageing induced mitochondrial Ca^{2+} overload is coupled with defects in SR Ca^{2+} homeostasis and loss of phosphorylation of phospholamban (pPLB) protein. Panel A, Histogram presenting mitochondrial Ca^{2+} ($[\text{Ca}^{2+}]_{\text{Mit}}$) in the young and old group, measured in 4- $\mu\text{mol/L}$ Fluo4-AM Ca^{2+} dye loaded (45-min) left ventricular cardiomyocytes. Panel B, Representative transient $[\text{Ca}^{2+}]_i$ changes under electrical stimulation (Left panel) and the amplitude of transient $[\text{Ca}^{2+}]_i$ changes (Right panel). Panel C, Corresponding kinetics of transient $[\text{Ca}^{2+}]_i$ changes (TP: the time to the maximum amplitude of $[\text{Ca}^{2+}]_i$ and RT_{50} : the half time of re-uptake of $[\text{Ca}^{2+}]_i$) in aged cardiomyocytes compared with those of young's. Panel D, Assessment of sarcoplasmic reticulum (SR) Ca^{2+} -content obtained following 10-mmol/L caffeine applications. Panel E, Western blot analysis for total PLB and pPLB levels; Actin served as the equal loading control. Panel F, Histogram presents fold-change in total PLB and pPLB levels. Data are derived from cardiomyocytes isolated from 5-6 rats/groups. Data presents the Mean \pm SEM values of the groups. Statistical significance * $P < 0.05$ vs. young group, analysed by unpaired two-sided Student's *t* test

higher in aged cardiomyocytes compared with the younger cardiomyocytes. Moreover, we observed an increase in basal levels of cytosolic free Na^+ ($[\text{Na}^+]_i$) and H^+ ($[\text{H}^+]_i$), measured as SNARF-1 intensity changes, in the aged cardiomyocytes, Figure 4 panels B-C.

We previously have shown in a rat model of insulin-resistance (MetS) that ionic balance was disrupted in an SGLT2 dependent manner.⁸ Therefore, we assessed whether age-related abnormalities in ionic balance were related to the deregulated expression of SGLT2. We assessed SGLT2 mRNA and protein expression in young and aged cardiomyocytes. As shown in Figure 4 panels D,E, the mRNA and protein levels of SGLT2 were significantly higher in aged cardiomyocytes.

To validate the possible correlation with SGLT2 activation and insulin resistance in left ventricular aged cardiomyocytes, we performed an oral glucose tolerance test (OGTT) in aged and young rats. As shown in Figure 4 panel F, the peak blood glucose levels measured at 30, 60 and 120 minutes were significantly higher in the aged rats compared with corresponding young rats. The HOMO-IR index was also high in the aged rats compared with the young rats (data not shown).

3.5 | Inhibition of SGLT2 rescues phosphorylation of PLB and suppress age-associated mitochondrial Ca^{2+} , $[\text{Ca}^{2+}]_{\text{Mit}}$ load in ventricular cardiomyocytes

Next, we assessed whether age-related defects in Ca^{2+} homeostasis were driven by SGLT2 activation. We monitored the effect of SGLT2 inhibition (incubation with dapagliflozin; 100 nmol/L for 4-5 hours at 37°C) on critical proteins involved in SR function. For these studies, we determined the expression level of SR Ca^{2+} ATPase (SERCA2a), $\text{Na}^+/\text{Ca}^{2+}$ -exchanger (NCX), PLB and phospho-PLB (pPLB) in young and aged rats in the absence and presence of SGLT2 inhibitor. As shown in Figure 5 panels A,B, there was no significant change in SERCA2a and NCX protein levels between young, aged and SGLT2 inhibited aged cardiomyocytes. Notably, Ca^{2+} handling defects in aged cardiomyocytes were consistent with the down-regulation of phosphorylated PLB (pPLB), a protein responsible for SERCA function, which was markedly recovered by inhibition of SGLT2, Figure 5 panels A and C. Also, SGLT2 inhibition reduced mitochondrial Ca^{2+} ($[\text{Ca}^{2+}]_{\text{Mit}}$) load in aged cardiomyocytes (Figure 5 panel D). Taken together, these data highlight an important role for SGLT2 in disrupting

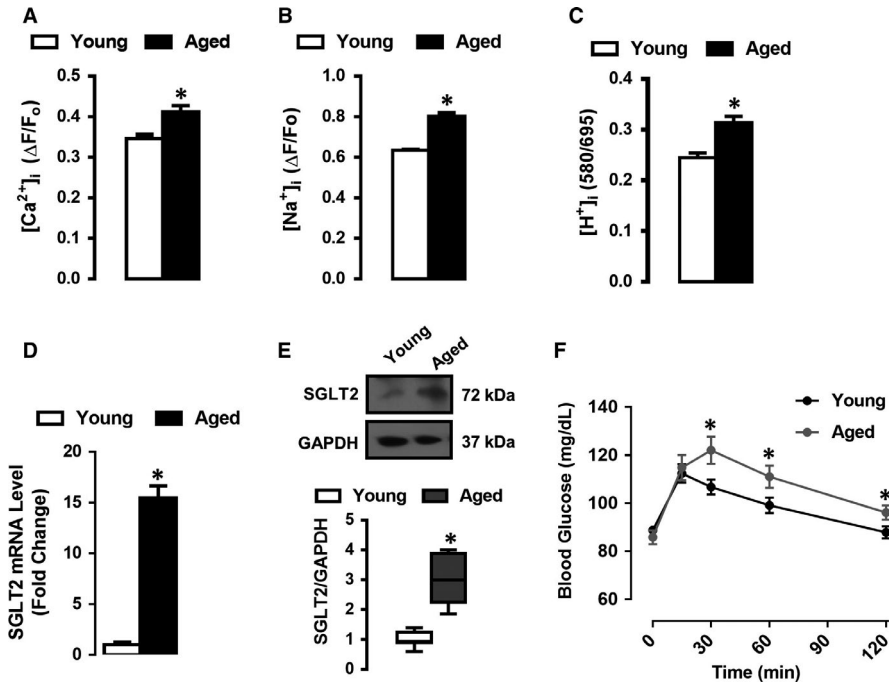


FIGURE 4 Sodium/Glucose co-transporter 2 (SGLT2) up-regulation increases resting levels of cytosolic ions in the aged left ventricular cardiomyocytes. The histogram presents Mean \pm SEM values of resting cytosolic ions shown in Panel A, cytosolic Ca^{2+} ($[\text{Ca}^{2+}]_i$), Panel B, cytosolic Na^+ ($[\text{Na}^+]_i$) and Panel C, cytosolic H^+ ($[\text{H}^+]_i$), detected in the cells loaded with either Ca^{2+} -sensitive Fura2-AM, Na^+ -sensitive SBFI fluorescent dye or H^+ -sensitive 5- $\mu\text{mol/L}$ SNARF-1 in young and aged cardiomyocytes. Cardiomyocytes were isolated from 5-6 rats/groups. Panel D, The mRNA levels of SGLT2 in isolated cardiomyocytes from young and old animals. Panel E, Western blot analysis of SGLT2 protein, GAPDH was used as the housekeeping gene. Panel F, The oral glucose tolerance test level, OGTT, of the aged rats compared with those of young's ($n = 10$ per group). The statistical significance level was $^*P < 0.05$ vs. young group, analysed by the unpaired two-sided Student's t test

Ca^{2+} homeostasis at the level of SR and mitochondria in the aged cardiac myocytes; inhibition of SGLT2 can restore the SR Ca^{2+} re-uptake and prevent Ca^{2+} build up in mitochondria of the aged cardiomyocytes.

3.6 | Inhibition of SGLT2 suppress NaK/NCX activity and restores $[\text{Ca}^{2+}]_i$ -homeostasis in aged cardiomyocytes

As significantly higher $[\text{Ca}^{2+}]_i$ and $[\text{Na}^+]_i$ were observed in aged cardiomyocytes with increased SGLT2 activity, we examined whether SGLT2 influences Na^+/K^+ -pump (NaK) or NCX activity. Interestingly, we observed a twofold increase in NaK current (I_{NaK}) in the aged cardiomyocytes compared with corresponding young hearts, Figure 6 panel A. Furthermore, we observed a similar increase in the NCX -currents in both forward and reversed directions (I_{NCXin} and I_{NCXout} , respectively) in the aged cardiac myocytes, Figure 6, panel B. Notably, the SGLT2 inhibitor dapagliflozin (100 nmol/L) restored I_{NaK} and I_{NCX} currents, respectively, in the aged cardiomyocytes highlighting the importance of SGLT2 in the regulation of intracellular ion-exchange currents, Figure 6 panels A,B.

Given these findings, we examined the effects of inhibition of SGLT2 on action potential (AP) prolongation in aged cardiac myocytes. As shown in Figure 6 panel C, SGLT2 inhibition

significantly improved AP repolarization in the aged cardiomyocytes. Furthermore, SGLT2 inhibition improved recovery of depressed Ca^{2+} -release, indicated by a significant recovery in the amplitude of $[\text{Ca}^{2+}]_i$ under electrical-field stimulation in aged cardiomyocytes (Figure 6 panel D). Collectively, these findings substantiate the involvement of SGLT in the regulation of SR and mitochondrial Ca^{2+} homeostasis during ageing.

4 | DISCUSSION

Ageing is a major factor that predisposes cardiac myocytes to metabolic and contractile abnormalities that leads to heart failure. Lipid peroxidation, oxidative stress and mitochondrial injury are central features of insulin resistance and obesity associated with advanced age.³¹⁻³³ Notably, mitochondrial perturbations, coupled with abnormalities in SR Ca^{2+} dysfunction have been identified as important contributors to the metabolic derangements with the ageing process in muscle cells.³⁴⁻³⁶ Herein, we provide new important evidence for the involvement of the sodium/glucose transporter, SGLT2 as a key regulator of cellular $[\text{Ca}^{2+}]_i$ homeostasis and age-associated cardiac dysfunction. Our data demonstrate that ventricular cardiomyocytes isolated from aged-rat hearts display mitochondrial abnormalities such as increased production of mitochondrial ROS and $[\text{Ca}^{2+}]_{\text{Mit}}$, reduced mitochondrial membrane potential (MMP) and altered

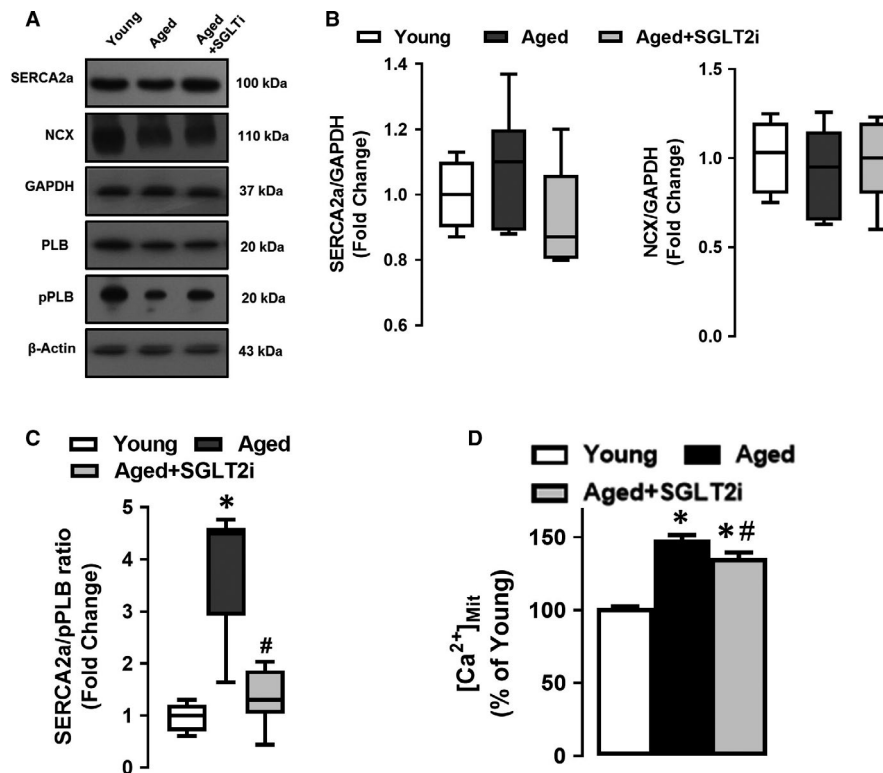


FIGURE 5 Inhibition of SGLT2 rescues phosphorylation of PLB and reduces mitochondrial Ca^{2+} load in the aged cardiomyocytes. Panel A, Western blot analysis of the lysate derived from young, aged and aged + SGLT inhibited (SGLT2i) cardiomyocytes for protein expression of sarcoplasmic reticulum Ca^{2+} -ATPase (SERCA2a), sodium/calcium-exchanger (NCX), GAPDH; total phospholamban (PLB) and phosphorylated (pPLB) and Actin. Panels B-C, Histogram presents fold change in SERCA2, NCX and pPLB levels of the younger group. Panel D, Histogram depicts the level of mitochondrial Ca^{2+} ($[\text{Ca}^{2+}]_{\text{Mit}}$) in Fluo4-AM loaded (4- $\mu\text{mol/L}$ for 45-min) young, aged and aged + SGLT inhibited (SGLT2i) cardiomyocytes. All data are presented as Mean \pm SEM, cardiomyocytes were isolated from 5-6 rats/groups. Statistical significance * $P < 0.05$ vs. young group, # $P < 0.05$ vs. aged group, analysed by the unpaired two-sided Student's t test

expression of mitochondrial quality control proteins. The underlying mechanism for ageing-associated increased ROS production is unclear. However, it may have resulted via an electron-transport leak from mitochondrial complex I or complex III associated with $[\text{Ca}^{2+}]_i$ -overload. Furthermore, carbonylation of respiratory electron transport chain proteins resulting in monoamine oxidase activity and mPTP opening from excess mitochondrial Ca^{2+} (increased $[\text{Ca}^{2+}]_{\text{Mit}}$) may also underline the ageing-associated increases in ROS production.³⁷ Furthermore, the role of oxidative stress in exacerbating mitochondrial health in aged cardiomyocytes is supported by our MitoTempo (antioxidant) data demonstrating that MitoTempo by suppressing mitochondrial ROS production prevented the loss of mitochondrial membrane potential (MMP) and normalized dynamics protein involved in fission and fusion. This view is consistent with a report showing $[\text{Ca}^{2+}]_{\text{Mit}}$ overload disrupted normal cardiac function.³⁸ Furthermore, we observed that Ca^{2+} signalling defects were not restricted to mitochondria. Our data also demonstrated a marked increase in cytosolic Ca^{2+} level ($[\text{Ca}^{2+}]_i$). This observation suggests that defects in intracellular Ca^{2+} signalling up-stream of mitochondria likely account for the observed increased $[\text{Ca}^{2+}]_{\text{Mit}}$. This view is concordant with a report suggesting that under conditions where $[\text{Ca}^{2+}]_i$ is high, the tendency of mitochondrial Ca^{2+} -uptake can increase by as much as 10- to 1,000-fold, resulting an overload in $[\text{Ca}^{2+}]_{\text{Mit}}$.⁶

In addition to $[\text{Ca}^{2+}]_i$, we also observed a marked increase in basal $[\text{Na}^+]_i$ in aged cardiomyocytes. The increased basal $[\text{Ca}^{2+}]_i$, in this case, maybe in part because of the depressed activity of PLB or leaky-RyR2.^{39,40} Consistent with this interpretation, we and others demonstrated that both depressed phospho-PLB and high frequency of Ca^{2+} -sparks with high gating properties can contribute to the high $[\text{Ca}^{2+}]_i$ in aged cardiomyocytes. Furthermore, we observed high basal levels of $[\text{Na}^+]_i$ in aged cardiomyocytes with higher NCX activities detected both in forward and reverse directions. If NCX is operationally higher in reverse mode, this would permit high Na^+ -influx into cells, whereas in the forward mode would provide a major Ca^{2+} -efflux mechanism.^{25,39} Alternatively, the observed increased $[\text{Na}^+]_i$ could be because of the activation of SGLT2 in aged cardiomyocytes as we observed in our previous study in insulin-resistant MetS rats.⁸ Herein, we show that SGLT2 was highly activated in ventricular cardiomyocytes of aged rats. We further demonstrate that SGLT2 contributes to dearrangements in $[\text{Ca}^{2+}]_i$ and $[\text{Na}^+]_i$ in aged cardiomyocytes, as the SGLT2 inhibitor (dapagliflozin) normalized the age-induced defects on intracellular $[\text{Ca}^{2+}]_i$ and $[\text{Na}^+]_i$. As SGLT2 inhibition could confer significant protection against age-associated defects in intracellular ion levels, we believe that SGLT2, when activated during ageing, contributes to aberrant alterations in $[\text{Ca}^{2+}]_i$ and $[\text{Na}^+]_i$ in

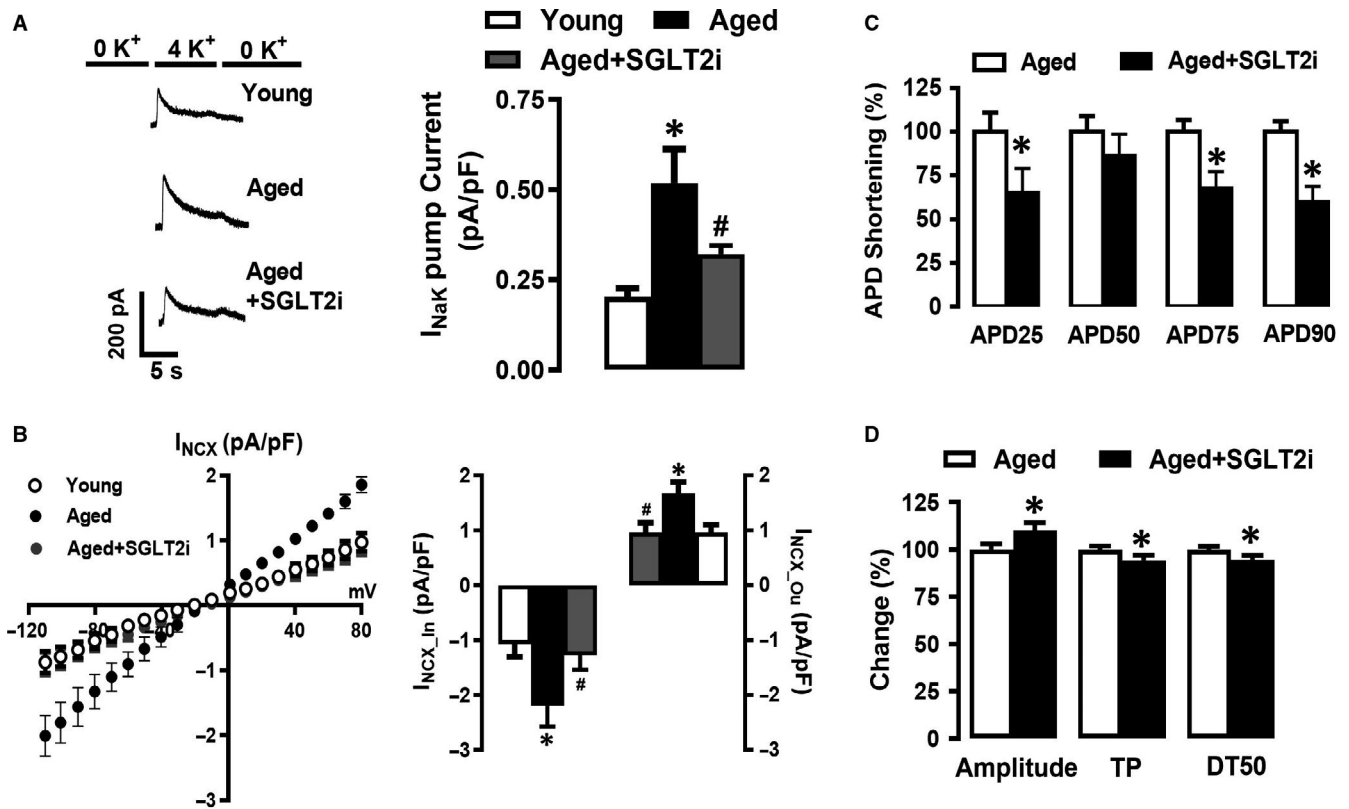


FIGURE 6 Inhibition of SGLT2 suppresses deregulated electrical activities of NaK and NCX and restores $[Ca^{2+}]_i$ -homeostasis in aged left ventricular cardiomyocytes. Panel A, Na^+/K^+ -pump currents (I_{NaK}) traces (left panel) in young, aged and aged + SGLT2 inhibited (SGLT2i) cardiomyocytes (treated with dapagliflozin; 100-nmol/L D185360; for 4-5 h), Right panel: Histogram presents Mean \pm SEM values for I_{NaK} current. Panel B, Left panel, shows Na^+/Ca^{2+} -exchanges currents (I_{NCX}) (inward; $I_{NCX_{in}}$ and outward; $I_{NCX_{ou}}$) and the maximum amplitudes of the currents, Right panel: Histogram presenting Mean \pm SEM values for NCX activity. Panel C, The effect of SGLT2 inhibition (SGLT2i) on prolonged AP repolarization phases in aged cardiomyocytes (measured at AP₂₅, AP₅₀, AP₇₅ and AP₉₀). The histogram presents Mean \pm SEM values, statistical significance * $P < 0.05$ vs. aged group. Panel D, SGLT2 inhibition provided important protection in the depressed Ca^{2+} -release and re-uptake (amplitude and time course of $[Ca^{2+}]_i$ changes such as TP: the time to the maximum amplitude of $[Ca^{2+}]_i$ and RT₅₀: the half time re-uptake of $[Ca^{2+}]_i$; left and right panels respectively) under electrical-field stimulation in the aged cardiomyocytes. The bar graphs present a per cent (%) change from the aged group. The statistical significance level was * $P < 0.05$ vs. aged group, analysed by unpaired two-sided Student's *t* test

cardiac myocytes. Our present data are in line with recent studies highlighting a role for SGLT2 inhibitors, on cardiometabolic, bioenergetics as well as the cardiac structure and NHE-1 activity.¹²⁻¹⁴ Previous, studies have shown that an increase in myocardial Na^+ level and Ca^{2+} level are a potential early drivers of death from cardiovascular diseases including heart failure, via induction of increased oxidative stress.¹⁵ Furthermore, it has also been shown that increased intracellular Na^+ can trigger mitochondrial ROS production in the diabetic heart through activation of SGLT2.^{14,16} Moreover, our present data demonstrating elevated levels of Na^+ , Ca^{2+} and H^+ in aged cardiomyocytes is concordant with previous studies which demonstrated normalization of the activated NHE-1 and increased intracellular Na^+ in cardiomyocytes under pathological conditions.^{12,13,16,17}

Our data highlight that de-regulated SGLT2 activity in cardiomyocytes promotes defective Ca^{2+} -handling that impairs contractile function with advanced age. This view is supported by recent clinical studies, demonstrating the use of metformin along with SGLT2 inhibition, in elderly patients.^{41,42} Further, several clinical

trials have demonstrated the beneficial effects of SGLT2 inhibitors on reducing cardiac morbidity risk of heart failure in the aged population.^{10-12,43}

Hence, our data suggest that deregulated SGLT2 during ageing disrupts mitochondrial function and cardiac contractility. Those effects seem to be associated with a mechanism that impinges upon deregulated $[Ca^{2+}]_i$ homeostasis. Our studies support the notion that interventions that modulate SGLT2 activity may provide benefits in maintaining $[Ca^{2+}]_i$ levels and cardiac function with advanced age. More importantly, our data demonstrate for the first time that ageing increases SGLT2 expression which negatively impacts mitochondrial/SR Ca^{2+} -homeostasis and cardiac function. In aggregate, our data provide novel evidence that SGLT2 is an important regulator of cardiac dysfunction with advanced age. Our studies further supported the notion that interventions that modulate SGLT2 activity may provide benefits in maintaining $[Ca^{2+}]_i$ levels and cardiac function with advanced age. Hence, targeted therapy for SGLT2 inhibition may prove beneficial in protection against age-associated contractile dysfunction.

ACKNOWLEDGEMENTS

The authors would like to thank Dr CV Bitirim (Stem cell Institute, Ankara University) for her help in flow cytometry.

CONFLICT OF INTEREST

No conflicts of interest, financial or otherwise, are declared by the authors.

AUTHOR CONTRIBUTION

Yusuf Olgar: Formal analysis (equal); Investigation (equal). **Erkan Tuncay:** Data curation (equal); Investigation (equal); Methodology (equal). **Sinan Degirmenci:** Investigation (equal). **Deniz Billur:** Investigation (equal). **Rimpy Dhingra:** Visualization (equal). **Lorrie Kirshenbaum:** Supervision (equal); Writing-review & editing (equal). **Belma Turan:** Conceptualization (equal); Funding acquisition (equal); Project administration (equal); Writing-original draft (equal).

DATA AVAILABILITY STATEMENT

The data used to support the findings of this study are available from the corresponding author upon reasonable request.

ORCID

Belma Turan  <https://orcid.org/0000-0003-2583-9294>

REFERENCES

- Strait JB, Lakatta EG. Aging-associated cardiovascular changes and their relationship to heart failure. *Heart Fail Clin*. 2012;8:143-164.
- Kirkwood TB. Understanding the odd science of aging. *Cell*. 2005;120:437-447.
- Payne BA, Chinnery PF. Mitochondrial dysfunction in aging: much progress but many unresolved questions. *Biochem Biophys Acta*. 2015;1847:1347-1353.
- Lee HY, Oh BH. Aging and arterial stiffness. *Circ J*. 2010;74:2257-2262.
- Tait SW, Green DR. Mitochondrial regulation of cell death. *Cold Spring Harb Perspect Biol*. 2013;5:1-15.
- Williams GSB, Boyman L, Chikando AC, Khairallah RJ, Lederer WJ. Mitochondrial calcium uptake. *Proc Natl Acad Sci*. 2013;110:10479-10486.
- Mammucari C, Rizzuto R. Signaling pathways in mitochondrial dysfunction and aging. *Mech Ageing Dev*. 2010;131:536-543.
- Durak A, Olgar Y, Degirmenci S, Akkus E, Tuncay E, Turan B. A SGLT2 inhibitor dapagliflozin suppresses prolonged ventricular-repolarization through augmentation of mitochondrial function in insulin-resistant metabolic syndrome rats. *Cardiovasc Diabetol*. 2018;17:144.
- Lam CSP, Chandramouli C, Ahojja V, Verma S. SGLT-2 Inhibitors in heart failure: current management, unmet needs, and therapeutic prospects. *J Am Heart Assoc*. 2019;8:e013389.
- Pasternak B, Ueda P, Eliasson B, et al. Use of sodium glucose cotransporter 2 inhibitors and risk of major cardiovascular events and heart failure: Scandinavian register based cohort study. *BMJ (Clinical research ed)*. 2019;366:l4772.
- Cintra R, Moura FA, Carvalho LSF, et al. Inhibition of the sodium-glucose co-transporter 2 in the elderly: clinical and mechanistic insights into safety and efficacy. *Rev Assoc Med Bras (1992)*. 2019;65(1):70-86.
- Garg V, Verma S, Connelly K. Mechanistic insights regarding the role of SGLT2 inhibitors and GLP1 agonist drugs on cardiovascular disease in diabetes. *Prog Cardiovasc Dis*. 2019;62:349-357.
- Verma S, Rawat S, Ho KL, et al. Empagliflozin lincreases cardiac energy production in diabetes: novel translational insights into the heart failure benefits of SGLT2 inhibitors. *JACC Basic Transl Sci*. 2018;3:575-587.
- Baartscheer A, Schumacher CA, Wust RC, et al. Empagliflozin decreases myocardial cytoplasmic Na(+) through inhibition of the cardiac Na(+)/H(+) exchanger in rats and rabbits. *Diabetologia*. 2017;60:568-573.
- Kohlhaas M, Liu T, Knopp A, et al. Elevated cytosolic Na+ increases mitochondrial formation of reactive oxygen species in failing cardiac myocytes. *Circulation*. 2010;121:1606-1613.
- Lambert R, Srodulski S, Peng X, Margulies KB, Despa F, Despa S. Intracellular Na+ concentration ([Na+]i) is elevated in diabetic hearts due to enhanced Na+-glucose cotransport. *J Am Heart Assoc*. 2015;4:e002183.
- Uthman L, Baartscheer A, Schumacher CA, et al. Direct cardiac actions of sodium glucose Cotransporter 2 inhibitors target pathogenic mechanisms underlying heart failure in diabetic patients. *Front Physiol*. 2018;9:1575.
- Kauffman ME, Kauffman MK, Traore K, et al. MitoSOX-based flow cytometry for detecting mitochondrial ROS. *React Oxyg Species (Apex)*. 2016;2:361-370.
- McKenzie M, Lim SC, Duchen MR. Simultaneous measurement of mitochondrial calcium and mitochondrial membrane potential in live cells by fluorescent microscopy. *J Vis Exp*. 2017;1-6.
- Olgar Y, Degirmenci S, Durak A, et al. Aging related functional and structural changes in the heart and aorta: MitoTEMPO improves aged-cardiovascular performance. *Exp Gerontol*. 2018;110:172-181.
- Wang SQ, Huang YH, Liu KS, Zhou ZQ. Dependence of myocardial hypothermia tolerance on sources of activator calcium. *Cryobiology*. 1997;35:193-200.
- Liu B, Wang LC, Belke DD. Effect of low temperature on the cytosolic free Ca2+ in rat ventricular myocytes. *Cell Calcium*. 1991;12:11-18.
- Oliver AE, Baker GA, Fugate RD, Tablin F, Crowe JH. Effects of temperature on calcium-sensitive fluorescent probes. *Biophys J*. 2000;78:2116-2126.
- Rocchetti M, Besana A, Mostacciolo G, Ferrari P, Micheletti R, Zaza A. Diverse toxicity associated with cardiac Na+/K+ pump inhibition: evaluation of electrophysiological mechanisms. *J Pharmacol Exp Ther*. 2003;305:765-771.
- Ozdemir S, Bito V, Holemans P, et al. Pharmacological inhibition of na/ca exchange results in increased cellular Ca2+ load attributable to the predominance of forward mode block. *Circ Res*. 2008;102:1398-1405.
- Song M, Mihara K, Chen Y, Scorrano L, Dorn GW 2nd. Mitochondrial fission and fusion factors reciprocally orchestrate mitophagic culling in mouse hearts and cultured fibroblasts. *Cell Metab*. 2015;21:273-286.
- Ong SB, Subrayan S, Lim SY, Yellon DM, Davidson SM, Hausenloy DJ. Inhibiting mitochondrial fission protects the heart against ischemia/reperfusion injury. *Circulation*. 2010;121:2012-2022.
- Kuka S, Tatarkova Z, Racay P, Lehotsky J, Dobrota D, Kaplan P. Effect of aging on formation of reactive oxygen species by mitochondria of rat heart. *Gen Physiol Biophys*. 2013;32:415-420.
- Hunter DR, Haworth RA. The Ca2+-induced membrane transition in mitochondria. I. The protective mechanisms. *Arch Biochem Biophys*. 1979;195:453-459.
- Panel M, Ghaleh B, Morin D. Mitochondria and aging: a role for the mitochondrial transition pore? *Aging Cell*. 2018;17:e12793.

31. Bhashyam S, Parikh P, Bolukoglu H, et al. Aging is associated with myocardial insulin resistance and mitochondrial dysfunction. *Am J Physiol Heart Circ Physiol*. 2007;293:H3063-H3071.
32. Martin-Fernandez B, Gredilla R. Mitochondria and oxidative stress in heart aging. *Age (Dordr)*. 2016;38:225-238.
33. Seo AY, Joseph AM, Dutta D, Hwang JC, Aris JP, Leeuwenburgh C. New insights into the role of mitochondria in aging: mitochondrial dynamics and more. *J Cell Sci*. 2010;123:2533-2542.
34. Miura S, Saitoh SI, Kokubun T, et al. Mitochondrial-targeted antioxidant maintains blood flow, mitochondrial function, and redox balance in old mice following Prolonged Limb Ischemia. *Int J Mol Sci*. 2017;18:1897.
35. Ni R, Cao T, Xiong S, et al. Therapeutic inhibition of mitochondrial reactive oxygen species with mito-TEMPO reduces diabetic cardiomyopathy. *Free Radic Biol Med*. 2016;90:12-23.
36. Jin H, Kanthasamy A, Ghosh A, Anantharam V, Kalyanaraman B, Kanthasamy AG. Mitochondria-targeted antioxidants for treatment of Parkinson's disease: preclinical and clinical outcomes. *Biochem Biophys Acta*. 2014;1842:1282-1294.
37. Paggio A, Checchetto V, Campo A, et al. Identification of an ATP-sensitive potassium channel in mitochondria. *Nature*. 2019;572:609-613.
38. Giorgi C, Baldassari F, Bononi A, et al. Mitochondrial Ca(2+) and apoptosis. *Cell Calcium*. 2012;52:36-43.
39. Zhu X, Bernecker OY, Manohar NS, et al. Increased leakage of sarcoplasmic reticulum Ca²⁺ contributes to abnormal myocyte Ca²⁺ handling and shortening in sepsis*. *Crit Care Med*. 2005;33:598-604.
40. Domeier TL, Roberts CJ, Gibson AK, Hanft LM, McDonald KS, Segal SS. Dantrolene suppresses spontaneous Ca²⁺ release without altering excitation-contraction coupling in cardiomyocytes of aged mice. *Am J Physiol Heart Circ Physiol*. 2014;307:H818-H829.
41. Hommers L, Fischer M, Reif-Leonhard C, Pfuhlmann B, Deckert J, Unterecker S. The combination of lithium and ACE inhibitors: hazardous, critical, possible? *Clin Drug Investig*. 2019;39:485-489.
42. Liao HW, Wu YL, Sue YM, Lee M, Ovbiagele B. Sodium-glucose cotransporter 2 inhibitor plus pioglitazone vs pioglitazone alone in patients with diabetes mellitus: a systematic review and meta-analysis of randomized controlled trials. *Endocrinol Diabetes Metab*. 2019;2:e00050.
43. Doumas M, Imprialos K, Stavropoulos K, Reklou A, Sachinidis A, Athyros VG. Combination of SGLT-2 inhibitors and GLP-1 receptor agonists: potential benefits in surrogate and hard endpoints. *Curr Pharm Des*. 2018;24:1879-1886.

SUPPORTING INFORMATION

Additional supporting information may be found online in the Supporting Information section.

How to cite this article: Olgar Y, Tuncay E, Degirmenci S, et al. Ageing-associated increase in SGLT2 disrupts mitochondrial/sarcoplasmic reticulum Ca²⁺ homeostasis and promotes cardiac dysfunction. *J Cell Mol Med*. 2020;24:8567-8578. <https://doi.org/10.1111/jcmm.15483>